

# On the Calculation of the Compton Profile in Crystalline LiH

K.-F. Berggren \*

FOA 4, Section 461, Fack, S-10450 Stockholm, Sweden

and

F. Martino

The City College of the City University of New York, New York, New York 10031

(Received 1 July 1970)

The Compton profile for LiH is calculated from a tight-binding wave function. The inclusion of the overlap between the hydrogen ions, previously neglected in the present context, is found to be important.

The development of high-resolution methods for the measurement of Compton x-ray scattering in solids<sup>1,2</sup> provides a particularly sensitive tool for investigating the momentum distribution of outer-shell electrons. It thus offers an independent test of the accuracy of theoretical band calculations, since the Compton profile appears to depend on the details of the valence-electron wave functions. In connection with recent measurements on crystalline LiH,<sup>2</sup> Phillips and Weiss have raised the question as to how accurate a calculation is necessary to obtain simultaneous agreement with such disparate quantities as Compton profile x-ray scattering factors, and total energies. Phillips and Weiss found that the valence-electron contribution to the measured profile in LiH is in marked disagreement with that calculated from the crystal-field wave functions of Hurst.<sup>3</sup> The observations indicate that the valence-electron momentum distribution is broader in momentum space than the distribution obtained from a superposition of H<sup>-</sup> and Li<sup>+</sup> wave functions for either the free ions or the H<sup>-</sup> ion in a Li<sup>+</sup>-point-lattice crystalline field. A further attempt to improve Hurst's wave functions by orthogonalizing the H<sup>-</sup> ion function to the Li<sup>+</sup> wave function produced no improvement in the calculation.

In the present paper we report on a calculation of the Compton profile in LiH using a tight-binding wave function which earlier has been found to give reasonable agreement with experiments for the cohesive energy and the equilibrium lattice parameter,<sup>4</sup> and the x-ray scattering factors.<sup>5,6</sup> Below we will show that the same wave function gives reasonable values for the Compton profile as well. This consistent picture is achieved by also including the overlap between the H<sup>-</sup> ions up to sufficient order. The wave functions of the H<sup>-</sup> ions are rather extended compared to the dimensions of the lattice, which results in large overlap integrals and a piling up of charge at the H<sup>-</sup> sites. As a consequence, the distribution in momentum space is broadened.

Given the  $n$ -electron wave function  $\Psi(\vec{r}_1, \vec{r}_2, \dots, \vec{r}_n)$ , the wave function in momentum space is defined by the transformation<sup>7</sup>

$$\Psi(\vec{p}_1, \vec{p}_2, \dots, \vec{p}_n) = (2\pi)^{-3n/2} \int d\vec{r}_1 d\vec{r}_2 \dots d\vec{r}_n \times \exp(-i \sum_{i=1}^n \vec{p}_i \cdot \vec{r}_i) \Psi(\vec{r}_1, \vec{r}_2, \dots, \vec{r}_n).$$

(Atomic units are used throughout this work.) We may define the momentum density as the expectation value

$$\rho(\vec{p}) = \langle \sum_{i=1}^n \delta(\vec{p} - \vec{p}_i) \rangle, \quad (2)$$

where the average is taken over the wave function in Eq. (1). Performing the integrations in Eq. (2), we may then express  $\rho(\vec{p})$  as

$$\rho(\vec{p}) = \frac{1}{(2\pi)^3} \int d\vec{r} \int d\vec{r}' e^{i\vec{p} \cdot (\vec{r} - \vec{r}')} \gamma(\vec{r}, \vec{r}'), \quad (3)$$

where  $\gamma(\vec{r}, \vec{r}')$  is the first-order density matrix in configuration space defined as<sup>8</sup>

$$\gamma(\vec{r}, \vec{r}') = n \int d\vec{r}_2 \dots d\vec{r}_n \Psi^*(\vec{r}', \vec{r}_2, \dots, \vec{r}_n) \times \Psi(\vec{r}, \vec{r}_2, \dots, \vec{r}_n). \quad (4)$$

Now the Compton scattering profile  $J(z)$  for a polycrystalline solid (where  $z$  is the initial component of momentum along the scattering vector) may be obtained from the spherical average  $\langle \rho(\vec{p}) \rangle_{av}$  of the momentum distribution by integration,<sup>1</sup>

$$J(z) = 2\pi \int_{|z|}^{\infty} \langle \rho(\vec{p}) \rangle_{av} p dp. \quad (5)$$

$J(z)$  is the quantity to be calculated below. By making the spherical average the anisotropy is ignored in the present calculation.

For an ionic crystal the first-order density matrix (4) is in the case of a single determinantal wave function with tight-binding orbitals given by<sup>9</sup>

$$\rho(\vec{r}, \vec{r}') = 2 \sum_{gh} \chi_g^*(\vec{r}') \Delta_{gh}^{-1} \chi_h(\vec{r}). \quad (6)$$

In Eq. (6),  $\chi_g$  are atomic functions centered at the different lattice sites, and  $\Delta_{gh}^{-1}$  are the elements of the inverse of the overlap matrix. The factor of 2 comes from the spin summation over doubly occupied orbitals. The choice of  $\Delta_{gh}^{-1} = \delta_{gh}$  in Eq. (6) corresponds to a superposition of free-ion solutions.

In the case of LiH we have in our calculations

assumed the simple electronic configuration  $\text{Li}^+(1s)^2 \text{H}^-(1s)^2$ , where the  $1s$  functions are the screened hydrogenic functions

$$\chi(\vec{r}) = (\alpha^3/\pi)^{1/2} e^{-\alpha r}. \quad (7)$$

The average momentum density is then, according to Eqs. (3) and (6),

$$\langle \rho(\vec{p}) \rangle_{\text{av}} = \frac{16}{\pi^2} \sum_{gh} \frac{(\alpha_g \alpha_h)^{5/2}}{(\alpha_g^2 + p^2)^2 (\alpha_h^2 + p^2)^2} \Delta_{gh}^{-1} \times \frac{\sin(p|\vec{R}_g - \vec{R}_h|)}{p|\vec{R}_g - \vec{R}_h|}. \quad (8)$$

In Eq. (8) the vectors  $\vec{R}_g$  define the lattice sites. Inserting the expression (8) in Eq. (5), we obtain the final expression for the Compton profile in LiH as

$$J(z) = J_{\text{H}^-}(z) + J_{\text{Li}^+}(z), \quad (9)$$

where

$$J_{\text{H}^-}(z) = \frac{32}{\pi} \sum_h \Delta_{\text{H}^-,h}^{-1} (\alpha_{\text{H}^-} \alpha_h)^{5/2} \times \int_{|z|}^{\infty} dp \frac{\sin(p|\vec{R}_{\text{H}^-} - \vec{R}_h|)}{|\vec{R}_{\text{H}^-} - \vec{R}_h|} \frac{1}{(\alpha_{\text{H}^-}^2 + p^2)^2 (\alpha_h^2 + p^2)^2} \quad (10)$$

and similarly for  $J_{\text{Li}^+}(z)$ . The normalization of  $J(z)$  is in accordance with Phillips and Weiss.<sup>2</sup> Eq. (9) seems to be a natural subdivision of the total Compton profile into the individual ion contributions.

The Compton profile, as defined in Eqs. (9) and (10), has been calculated numerically with  $\alpha_{\text{Li}^+} = 3 - \frac{5}{16} = 2.6875$  and with three different choices of  $\alpha_{\text{H}^-}$ , namely,  $\alpha_{\text{H}^-} = 1 - \frac{5}{16} = 0.6875$  (obtained from minimization of the energy of the free ions),  $\alpha_{\text{H}^-} = 0.7208$  (from minimization of the total crystal energy<sup>4</sup>), and  $\alpha_{\text{H}^-} = 0.77242$  (from Hurst's closed-shell crystal-field calculation<sup>3</sup>). In the calculations we have successively included shells up to the fourth order, i.e., 32 neighboring ions. In Fig. 1, we display the results for  $\alpha_{\text{H}^-} = 0.7208$ , noting that the two other choices for  $\alpha_{\text{H}^-}$  lead to unimportant changes. The curve (i) in Fig. 1 shows clearly the inadequacy of a superposition of a free-ion solutions in the present contest. The curve (ii) is the result of orthogonalizing the nearest unlike neighbor wave functions. As was noted by Phillips and Weiss,<sup>2</sup> this extension leads to an insignificant improvement. A major improvement [curve (iii)] in the calculated Compton profile appears when the overlap between nearest negative ions (second shell) is included. As shown by curve (iv) the inclusion of also the next nearest hydrogen ions (fourth shell) essentially confirms (iii). For this reason we have not carried the calculations further; with increasing distance

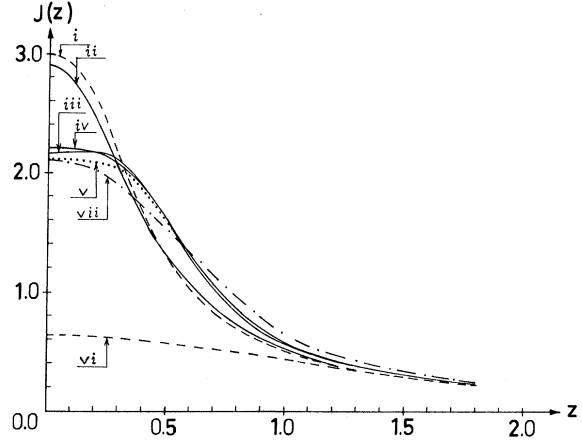


FIG. 1. Compton profiles for crystalline LiH (four electrons per LiH pair). Curve (i) corresponds to a plain superposition of ion solutions. In curve (ii) the nonorthogonality between the first unlike nearest neighbors is taken into account. In curves (iii) and (iv) the nonorthogonality is included up to the second and fourth shell, respectively. Curve (v) is the result of an orbital splitting with the fourth shell of neighbors included. Curve (vi) is the contribution from the  $\text{Li}^+$  free-atom  $(1s)^2$  core. Curve (vii) is the spherically averaged experimental results (Ref. 2).

$|\vec{R}_{\text{H}^-} - \vec{R}_g|$  the sine function in the integrand of Eq. (10) oscillates faster and the resulting integral is therefore small. It is noteworthy that the numerically important changes upon orthogonalization appear in  $J_{\text{H}^-}(z)$ . This is because of the large overlap between the hydrogen ions and the strong deformation of these ions when forming the crystal.

Incidentally, we have found a small but interesting improvement in the results above if the restraint of doubly occupied orbitals is relaxed and an orbital splitting of the up- and down-spin electrons at the hydrogen sites is allowed (also referred to as an open-shell configuration or unrestricted Hartree-Fock). In this case the formulas above should be supplemented with a summation over spin. The curve (v) in Fig. 1 has been calculated with the orbital exponents taken from Hurst's<sup>3</sup> open-shell crystal-field calculation, i.e.,  $\alpha_{\text{H}^-} = 1.0074$  for spin-up electrons, let us say, and  $\alpha_{\text{H}^-} = 0.57146$  for spin-down electrons. The improvement obtained from splitting the orbitals gives a hint that this type of correlation splitting might be a real effect.

In summary, we have shown that it is possible to calculate the Compton profile in LiH from a tight-binding wave function, if only the nonorthogonality between the hydrogen ions is taken into account properly. In view of the simple hydrogen-like orbitals chosen, the agreement with the experimental results is reasonable ( $\lesssim 10\%$ ). The tight-

binding wave function used also gives reasonable values for the cohesive energy and the lattice parameter<sup>4</sup> and the x-ray scattering factors.<sup>5,6</sup> The present calculations shows that the distribution in momentum space is broader than the one obtained from a superposition of free-ion solutions.  
*Note added in proof.* After the submission of this

work another calculation of the Compton profile in LiH has appeared [W. Brandt, Phys. Rev. B **2**, 561 (1970)]. The wave function of Brandt, Eder, and Lundqvist (Ref. 5) is also found to account in a satisfactory way for the measured Compton profile. We are indebted to Professor Werner Brandt for sending us a copy of his work.

\*Present address: Cavendish Laboratory, Cambridge, England (until Oct., 1971).

<sup>1</sup>W. C. Phillips and R. J. Weiss, Phys. Rev. **171**, 790 (1968).

<sup>2</sup>W. C. Phillips and R. J. Weiss, Phys. Rev. **182**, 923 (1969).

<sup>3</sup>R. P. Hurst, Phys. Rev. **114**, 746 (1959).

<sup>4</sup>S. O. Lundqvist, Arkiv Fysik **8**, 177 (1953). For the cohesive energy, Lundqvist reports -205 kcal/mole compared to observed -217 kcal/mole.

<sup>5</sup>I. Waller and S. O. Lundqvist, Arkiv Fysik **7**, 121 (1953); A. Westin, I. Waller, and S. O. Lundqvist, *ibid.* **22**, 371 (1962). See also the remarks on the calculation

of the x-ray scattering factors in W. Brandt, L. Eder, and S. O. Lundqvist, Phys. Rev. **142**, 165 (1966).

<sup>6</sup>R. S. Calder, W. Cochran, D. Griffiths, and R. D. Lowde, J. Phys. Chem. Solids **23**, 621 (1962). In Fig. 4 of this reference the experimental x-ray scattering factors are compared with the theoretical values of Waller and Lundqvist in Ref. 5.

<sup>7</sup>A. Messiah, *Mécanique Quantique* (Dunod, Paris, 1962), Vol. I, p. 107.

<sup>8</sup>P. O. Löwdin, Phys. Rev. **97**, 1474 (1955).

<sup>9</sup>P. O. Löwdin, Phys. Rev. **97**, 1490 (1955); Phil. Mag. Suppl. **5**, 1 (1956).

## ERRATA

Electronic Properties of Liquid Metals. N. W. Ashcroft and W. Schaich [Phys. Rev. B **1**, 1370 (1970)]. The following typographical errors have been found: In Eq. (39),  $-\delta_{i_1, i_2} \dots$  should be replaced by  $+\delta_{i_1, i_2} \dots$ ; in Eq. (40),  $-\delta_{i_1, i_2} \dots$  should be replaced by  $+\delta_{i_1, i_2} \dots$ ; Eqs. (51)–(53) should all include on the right-hand side an extra factor of  $(-\hbar^2/2mk_F)$  multiplying the derivative of  $s_i$ ; Eq. (56) should include a factor of  $v(x)$  in the second term on the right-hand side; Eq. (B6), instead of  $\frac{1}{2}\pi(2mk_F/\hbar) \dots$ , should have  $-\frac{1}{2}\pi(2m\tilde{k}_F/\hbar^2)$ ; and Eq. (B8), instead of a factor  $(1/\epsilon)$ , should have  $(i/\epsilon)$ . We have also discovered an algebraic error in Eq. (B11). Instead of the factor  $(-2i/3\pi Z)$ , one should have  $(-2/3\pi Z)$ . The definitions of the  $G^{12}$  and  $G^{21}$  [Eq. (42)] are then changed to

$$G^{21}(l_1, l_2) = G^{12}(l_1, l_2) = + (2/3\pi Z)(2l_1 + 1)^{1/2}(2l_2 + 1)^{1/2}.$$

These corrections substantially change the numerical results as presented in Sec. IV, Figs. 1–4, and Table I. For instance, the iterated resistivity [still within the muffin-tin approximation and using Eq. (49)] now appears to tend to 5.9, 1.15, and 4.7 times the experimental value for Na, Zn, and Al, respectively. The difficulty with the optical theorem is, however, almost eliminated. For further discussion of the corrected numerical results see W. Schaich, thesis, Cornell University, 1970 (unpublished).

Ge-Aqueous-Electrolyte Interface: Electrical Properties and Electroreflectance at the Fundamental Direct Threshold. D. E. Aspnes and A. Frova [Phys. Rev. B **2**, 1037 (1970)]. The numerical prefactor in Eq. (4.3), which relates the field-induced reflectivity change  $\Delta R/R$  to the field-induced change in the real part of the effective dielectric function  $\langle \Delta E_1 \rangle$ , should be 0.0432 instead of 0.0109 as shown in Eq. (4.3). This change does not affect the experimental electroreflectance data (given as  $\Delta R/R$  vs photon energy or electric field strength), or conclusions based on features of the experimental electroreflectance line shape. The theoretical amplitude predicted by each of the three simple models will change as follows.

In the low-field limit, the peak-to-peak amplitude of  $\Delta R/R$  predicted by the  $n=1$  exciton line, continuum exciton, and Franz-Keldysh models are now calculated to be  $72 \times 10^{-4}$ ,  $6.3 \times 10^{-4}$ , and  $1.25 \times 10^{-4}$ , respectively, compared to the experimentally observed value of  $7 \times 10^{-4}$  at this field ( $\mathcal{E}_s = 1000$  V/cm). In the high-field limit, the discrepancy between experimental measurement and the predictions of the Franz-Keldysh theory modified by the field inhomogeneity is now 3 to 4 instead of 13 to 15, with the experimental number being larger.

This correction does not change the main conclusion of this section: that experimentally observed changes in  $\Delta R/R$  are much too large to be described by the Franz-Keldysh mechanism, and